This is an *Accepted Manuscript*, which has been through the Royal Society of Chemistry peer review process and has been accepted for publication.

Accepted Manuscripts are published online shortly after acceptance, before technical editing, formatting and proof reading. Using this free service, authors can make their results available to the community, in citable form, before we publish the edited article. We will replace this *Accepted Manuscript* with the edited and formatted *Advance Article* as soon as it is available.

You can find more information about *Accepted Manuscripts* in the **Information for Authors**.

Please note that technical editing may introduce minor changes to the text and/or graphics, which may alter content. The journal's standard **Terms & Conditions** and the **Ethical guidelines** still apply. In no event shall the Royal Society of Chemistry be held responsible for any errors or omissions in this *Accepted Manuscript* or any consequences arising from the use of any information it contains.

Journal Name

ARTICLE TYPE

Isoquinoline-based Werner clathrates with xylene isomers: Aromatic interactions vs. molecular flexibility

**Merrill M. Wicht,[a,b] Nikoletta B. Báthori*[b] and Luigi R. Nassimbeni[a]**

The crystal structures of the Werner clathrates $Ni(NCS)_2(isoquinoline)_4$ (**H**) with *para*-xylene (**px**), *meta*-xylene (**mx**) and *ortho*-xylene (**ox**) have been elucidated. The kinetics of thermal decomposition of the three inclusion compounds were performed using the isothermal technique of Flynn and Wall. Selectivity of **H** for the xylene isomers was determined for both the liquid and vapour phase binary mixtures of the
10 xylenes. The chosen ligand has a larger aromatic system to improve the possible π interactions between **H** and the selected guests. The planarity of the isoquinoline ligand causes **H** rigidity and its selectivity was compared to a related Werner complex containing the more flexible 4-phenylpyridine.

Introduction

Werner clathrates are inclusion compounds of general formula
15 $MX_2L_4 \cdot nG$, where M is a divalent metal cation (typically Ni(II), Co(II), Fe(II), Cu(II) and Mn(II)), X is an anionic ligand (NCS^-, NCO^-, CN^-, NO_3^- or halide), L is a substituted pyridine or α-arylalkylamine, and G is a Guest, usually an organic aromatic compound. They have the ability to absorb organic compounds
20 reversibly, and the first experimental studies of this phenomenon were carried out by Schaeffer and co-workers in 1957.[1] Lipkowski has studied various physico-chemical aspects of these compounds, including their selectivity, crystal structures, and the thermodynamics of sorption and kinetics of desorption, and these
25 have been summarised in reviews.[2,3] In the well-studied Werner complex [Ni(NCS)_2(4-methylpyridine)_4] the two anionic ligands are in *trans* positions to each other and steric hindrance between the pyridine ligands results in a 'four-blade propeller' arrangement around the central metal ion. Noted in these studies
30 is the dependence of lattice expansion on the volume and shape of the guest molecules. In most cases the host:guest ratio is 1:1. Physical properties of these structures are dependent on both the packing of the hosts as well as the kind of properties of the guest. The enthalpy of clathration is related to the cavities in the host
35 lattice.[3] Soldatov[4] revisited the host compound [Ni(NCS)_2(4-methylpyridine)_4] and determined three crystal structures: dense (*α*), microporous (*β*) polymorphs and *γ*-inclusion phases. The adaptability of this host towards guest compounds is attributed to the fact that its *β*-phase volume expands by 5 – 14% upon guest
40 inclusion. Recently there has been renewed interest in Werner clathrates[5,6] and Lusi and Barbour[7] have described polymorphism associated with an order-disorder phase transition of the guest in the [Ni(NCS)_2(4-phenylpyridine)_4] clathrate dependent on the thermal range investigated. The host preferentially discriminated
45 in favour of one of the three isomers of xylene in solid-vapour competition experiments[8] and Batisai and co-workers[9] explored

the preparation of phases by mechanochemical techniques which resulted in a series of solid solutions. Different sorption properties were exhibited by these solid solutions compared with
50 the pure Werner complexes. Recently the structures of three Werner complexes have been analysed in terms of their packing, and the results of crystal densities were justified by Hirshfeld surface analysis and density functional theory calculations.[10]

In this work we present the structures, thermal decomposition
55 kinetics and the selectivity of the Werner host [Ni(NCS)_2(iso-quinoline)_4, **H**] with *para*-, *meta*- and *ortho*-xylene (**px**, **mx** and **ox**, respectively). The ligand isoquinoline has a fused ring structure which according to the Cambridge Structural Database[11], has previously only been encountered once as a
60 ligand in Werner clathrates[12] but its selectivity was not investigated. This ligand was chosen because its two fused rings give it a large aromatic surface area which is important for C-H···π and π···π host:guest interactions. The structural line diagrams and atomic numbering scheme for the **H** and the xylene
65 guests are shown in Scheme 1.[13]
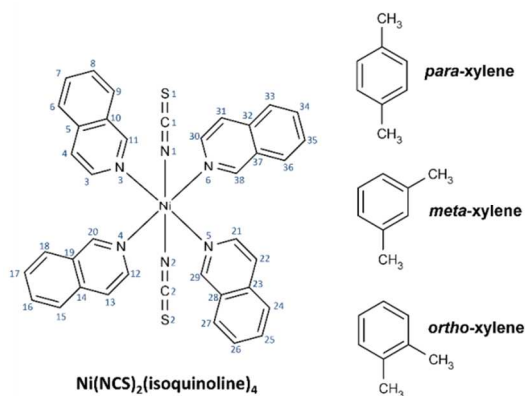
Scheme 1 Structural line diagrams and atomic numbering scheme of the host, $Ni(NCS)_2(isoquinoline)_4$, and the xylene isomers

Results and discussion

Crystal structures of H·px, H·mx and H·ox

The structure of **H·px** was solved in the hexagonal space group
5 $P6_1$ (No. 169) and the details of the data collection and refinement are summarised in Table 1. The asymmetric unit consists of one host and one guest molecule (Fig.1a). The host is positioned in *Wyckoff* position *a* and severely disordered. Two of the isoquinoline ligands lying trans across the Ni centre are
10 disordered and eventually were modelled with 50% site occupancy. The final model of the ligand had refined the C and N atoms anisotropically and the H atoms with the usual riding model. The other two isoquinoline ligands and the thiocyanate groups were ordered and refined uneventfully. The atomic
15 positions of the **px** guest were located unequivocally from the difference electron density map. However, convergence of the refinement could only be achieved with the guest treated isotropically with appropriate bond length constraints. The ordered **px** molecules are situated in cavities (Fig. 1b, **px** is
20 presented with spacefill model, red) and form a helical arrangement along the *c* axis.

The **H·mx** structure displays similar features with the **H·px** and crystallised in the $P6_5$ (No. 170) space group. The asymmetric unit contains one host and one guest and the host positoned in
25 *Wykoff* position *a*. In a similar manner to **H·px,** the host has two ordered and two disordered isoquinoline ligands which were refined with 50% S.O.Fs (Fig 1c). The **mx** guest is ordered and positioned in cavities (Fig. 1d) and the packing is enantiomeric with **H·px**.

30 The structure of **H·ox** was solved in the monoclinic *C2/c* (No. 15) space group. One host molecule is in a general position (*Wykoff f*) and one is located in a diad (*Wyckoff e*). Similarly one guest is on a general position and the second guest is on a centre of inversion (*Wyckoff b*), thus the asymmetric unit is composed of 1.5 host and
35 1.5 guest molecules (Fig. 1e). The host molecule in the general position has one of its four isoquinoline ligands disordered and

refining to S.O.Fs 77% and 23%. The host molecule in a special position with two of its ligands situated on a diad. Both the ordered (Fig. 1f, molecule A, yellow) and the disordered guest
40 (Fig. 1f, molecule B, green) are located in cavities. The structure shows remarkable similarity with **H·px** and **H·mx** from [100] direction.

The intermolecular interactions between the xylene guests and the host framework were analysed using the program Crystal
45 Explorer[14] which calculates the Hirshfeld surface[15] of a target molecule in a crystal structure and depicts all its interactions with the neighbouring molecules. Fig. 2a shows the **px** guest covered by its Hirshfeld surface when surrounded by host molecules and the generated fingerprint plot,[16] the 2D representation of the 3D
50 surface. The red areas on the surface indicate C-H⋯π close contacts between the **px** and the hosts. The fingerprint plot was generated using one pair of the two disordered isoquinoline moieties. The resulting plot, generated by using the alternative pair of ligands, is very similar. The C⋯H contacts are
55 highlighted in blue, and comprise ca. 48% of the interactions. The upper lobe, labelled ①, represents close contacts between the **px** hydrogens to the aromatic system of the host, while the lower lobe ② shows the contacts between the hydrogens of the ligands and the aromatic region of the **px**. The structure also displays a
60 number of C-H⋯π interactions between the host molecules. Fig. 2b displays the **mx** guest in its Hirshfeld surface and the corresponding fingerprint plot shows a similar environment for the guest to the **H·px** structure with ca. 47% C⋯H contacts. In case of **H·ox**, the disordered guest was not analysed. The
65 Hirshfeld surface of the ordered guest shows less intensive interactions with the nearby hosts (smaller area on Fig. 2c). This corresponds to the amount of observed C⋯H contacts (ca. 44%) and their generally longer nature. Interestingly there are significant (**ox**)C-H⋯S(host) contacts with (d_i+d_e)= 2.7Å. This
70 type of hydrogen bonding has previously been identified by Đaković et al. in Ni(II) complexes.[17]
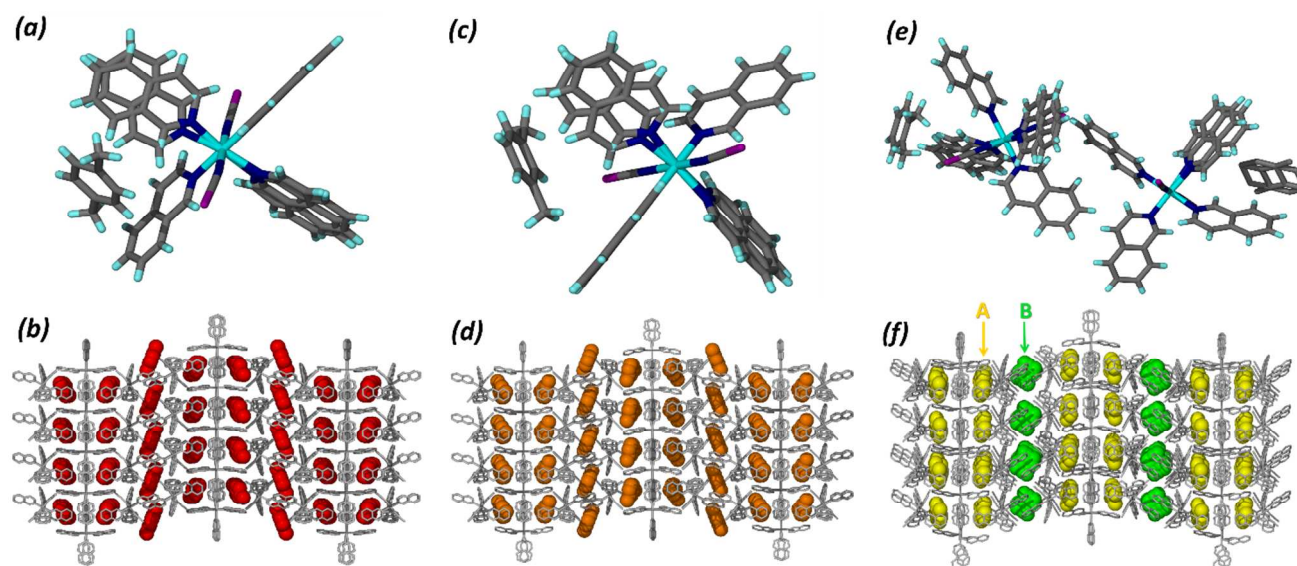
Fig. 1 Structural comparison of **H·px** (a- molecular structure, b- packing viewed down *a*, **px** is presented with spacefill model, red), **H·mx** (c- molecular
75 structure, d- packing viewed down *a*, **mx** is presented with spacefill model, orange) and **H·ox** (e- molecular structure, f- packing viewed down *a*, **ox** is presented with spacefill model, yellow and green)

Journal Name

ARTICLE TYPE

Table 1 Crystallographic data for **H·px**, **H·mx** and **H·ox**.

.	H·px	H·mx	H·ox
Chemical Formula	$Ni(NCS)_2(C_9H_7N)_4.C_8H_{10}$	$Ni(NCS)_2(C_9H_7N)_4.C_8H_{10}$	$Ni(NCS)_2(C_9H_7N)_4.C_8H_{10}$
Host:guest ratio	1:1	1:1	1:1
Formula Weight	797.65	797.65	1199.50
Temperature/K	173(2)	173(2)	173(2)
Crystal System	Hexagonal	Hexagonal	Monoclinic
Space Group (no.)	$P6_1$ (no. 169)	$P6_5$ (no. 170)	$C2/c$ (no. 15)
a/Å	10.7810(15)	10.8390(15)	10.671(2)
b/Å	10.7810(15)	10.8390(15)	19.132(4)
c/Å	59.780(12)	59.167(12)	59.609(12)
α/°	90.00	90.00	90.00
β/°	90.00	90.00	91.49(3)
γ/°	120.00	120.00	90.00
V/A^3	6017.3(17)	6019.9(17)	12166(4)
Z/Z	1/6	1/6	1.5/12
D_{calc}/Mg.m^{-3}	1.321	1.320	1.310
Radiation type	MoKα	MoKα	MoKα
F(000)	2496	2466	2016
Crystal size/mm	0.41 x 0.45 x 0.51	0.24 x 0.26 x 0.53	0.080 x 0.190 x 0.340
Colour, crystal form	Blue, octahedral	Blue, octahedral	Blue, octahedral
No. of total reflections	8794	5150	9660
No. of unique reflections	7094	4048	7315
$\Theta_{min-max}$/°	2.04/ 27.12	12.00/ 26.89	2.13/ 27.26
$R[F^2>2\sigma(F^2)],wR(F^2), S$	0.0692, 0.1963, 1.017	0.0461, 0.1055, 1.028	0.0686, 0.1639, 1.061
No. of parameters/data	637/8794	667/5150	893/9660
Res.peak (max/min)/e A^{-3}	1.0102/-0.723	0.229/ -0.166	0.796/ -0.622

5
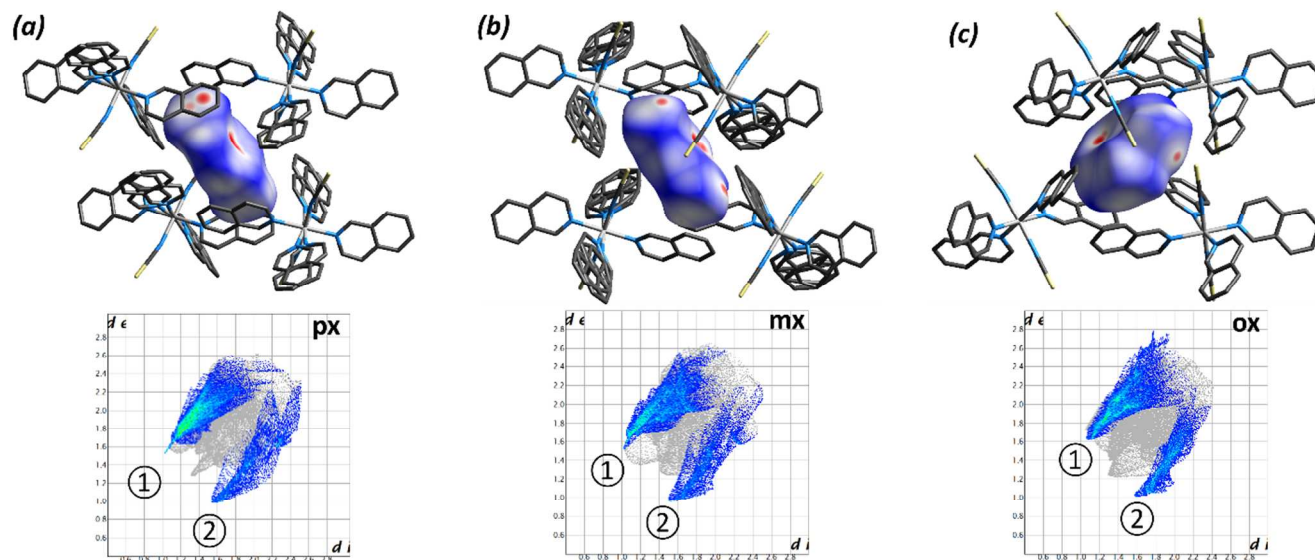
Fig. 2 Hirshfeld surfaces and their fingerprint plots of **px** (a), **mx** (b) and **ox** (c, ordered guest only); ① indicates close contacts between the guest hydrogens to the aromatic system of the host, while ② shows the contacts between the ligand hydrogens and the aromatic region of the guest.

10

ARTICLE TYPE

Kinetics of thermal decomposition

The kinetics of thermal decomposition of all three inclusion compounds were carried out by the non-isothermal technique of Flynn and Wall.[18] Desorption curves were recorded at fixed
5 heating rates β = 2, 4, 8, 16 and 32 K min^{-1} for all three clathrates. A set of curves for **H·px** is shown in Fig. 3. The decomposition takes place in three distinct steps. **Step 1** represents the disintegration of the inclusion compound via loss of the guest. This step is calculated as a 13.3% loss in mass. **Step 2** and **Step 3**
10 correspond to the decomposition of the host, in each step the mass loss of two isoquinoline ligands at a percentage loss of 32.4% each. The decomposition curves of **H·mx** and **H·ox** are similar and have been deposited in the Electronic Supplementary Information (ESI, Fig. S1 and S2). The calculated and
15 experimental TG results for **H·px**, **H·mx** and **H·ox** are summarised in Table 3.
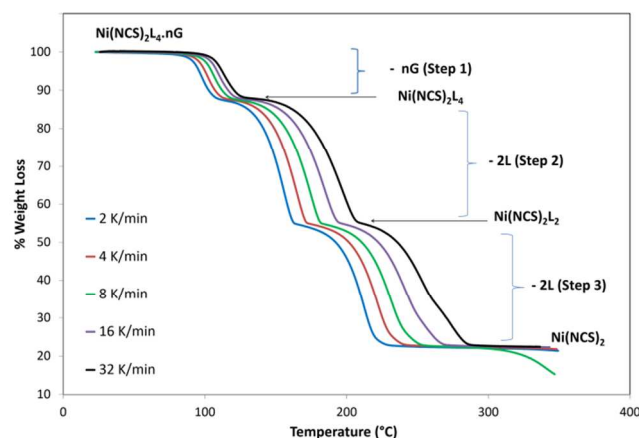
Fig. 3 Non-isothermal TG curves for **H·px**

20

Table 3 Thermal analysis results for **H·px**, **H·mx** and **H·ox**

Compound	H·px Exp (Calc) %	H·mx Exp (Calc) %	H·ox Exp (Calc) %
Mass Loss			
Step 1	13.1 (13.3)	13.1 (13.3)	13.2 (13.3)
Step 2	32.3 (32.4)	32.1 (32.4)	31.8 (32.4)
Step 3	32.1 (32.4)	31.8 (32.4)	32.1 (32.4)

For **Step 1** the mass loss corresponding to the loss of 1 mole of guest and activation energy were calculated over α ranges for
25 each of the three inclusion compounds and are indicated in Table 4. The extent of reaction, is defined as

$$\alpha = (m_t - m_0)/(m_\infty - m_0)$$

with m_0 = initial mass, m_t = mass at time t and m_∞ = final mass. Plots of log β/β_0 vs 1/T for the **H·px** where β is the heating rate are given in Fig.4. The activation energies for α positions 0.2, 0.5

30 and 0.75 of **Step 1** are illustrated in Fig. 4a. Similarly, **Step 2** at α positions 0.2, 0.5 and 0.8 and **Step 3** at α positions 0.3, 0.45 and 0.6 are demonstrated in Fig. 4b and 4c, respectively. Activation energies were calculated from the slopes:

$$slope = -0.457\frac{E_a}{R}$$

35 The activation energies for the three thermal decomposition steps for each compound are shown in Table 4. Graphical information for **H·mx** and **H·ox** has been deposited in the ESI (Fig. S3 and S4).

Step 1 decomposition reaction required the largest activation
40 energy. The activation energy for **Step 2** is the lowest for the three steps and is 105-108 for **H·px,** 103-116 for **H·mx** and 93-100 kJ.mol^{-1} for **H·ox**. The higher values of the activation energies associated with the loss of the volatile xylene guests can be justified in terms of the topologies of the structures of the
45 clathrates. In each case the xylene guest is trapped in a cavity, thus requiring a severe disruption of the host framework in order to release the guest. The effect of topology on the thermal stability and kinetics of decomposition of inclusion compounds has been reviewed[19] and, in general, structures that may be
50 described as intercalates are less stable than tubulates which, in turn are less stable than cryptates. The latter often have higher activation energies of desorption.

Table 4 Activation energy ranges for thermal decomposition (kJ.mol^{-1})

Reaction Step	H:ox	H:mx	H:px
Step 1	138-142	170-177	178 - 192
Step 2	93-100	103-116	105 - 108
Step 3	112	118-120	115 - 120

55
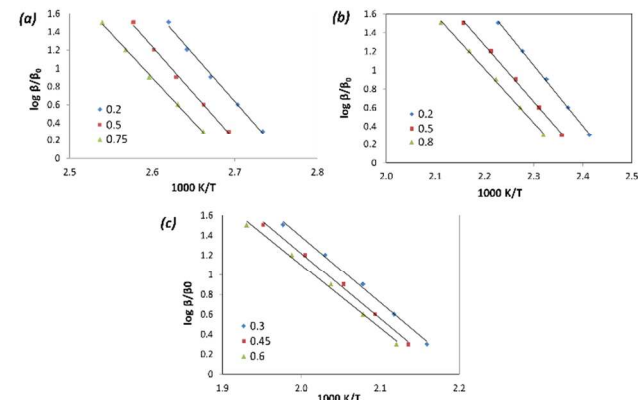
Fig. 4 Activation energies for (a) **Step 1**, (b) **Step 2** and (c) **Step 3** for **H·px**

60

Selectivity experiments

Experiments to determine the selectivity profile of this host were carried out by two methods. Firstly by dissolving the host in liquid mixtures of the guests with known proportions and
5 harvesting the crystals of the ensuing inclusion compounds for analysis; secondly by exposing the powdered apohost to mixtures of the guest vapours (solid vapour sorption) and subsequent analysis by headspace gas chromatography. These competition experiments between pairs of xylene isomers (**ox/px**, **ox/mx** and
10 **mx/px**) were performed at different ratios (0:1; 0.2:0.8; 0.4:0.6; 0.6:0.4; 0.8:0.2 and 1:0). The crystals were harvested, dried and lightly crushed for analysis.

When a host compound is crystallised from a mixture of two guests A and B to form a crystal containing a ratio of the two
15 guests (H·n'A·m'B), the selectivity coefficient of this competition experiment can be determined from the formula

$$K_{A:B} = (K_{B:A})^{-1} = Z_A/Z_B * X_B/X_A \qquad (X_A + X_B = 1)$$

where X_A, X_B are the mole fractions of the guests in the mother liquor and Z_A, Z_B are their mole fractions in the crystal. The
20 results of the competition experiments are shown in Fig. 5 in which the mole fraction of a given guest in solution (X_{guest}) is plotted against its mole fraction in the solid state (Z_{guest}). In Fig. 5a a small amount of preference is shown for **ox** over **px** for the composition mixture of **ox/px.** Fig. 5b indicates the selectivity of
25 **ox** compared with **mx** in the crystal structure with the host shows no preference for one over the other. Similarly in Fig. 5c there is no preference for the host to enclathrate one of **mx** or **ox** over the other. Selectivity for both procedures (crystallisation and solid-vapour sorption) is shown graphically and no preference for
30 either of the two xylenes is observed. That is, in all three cases poor selectivity is found for one of the isomers over the other two.
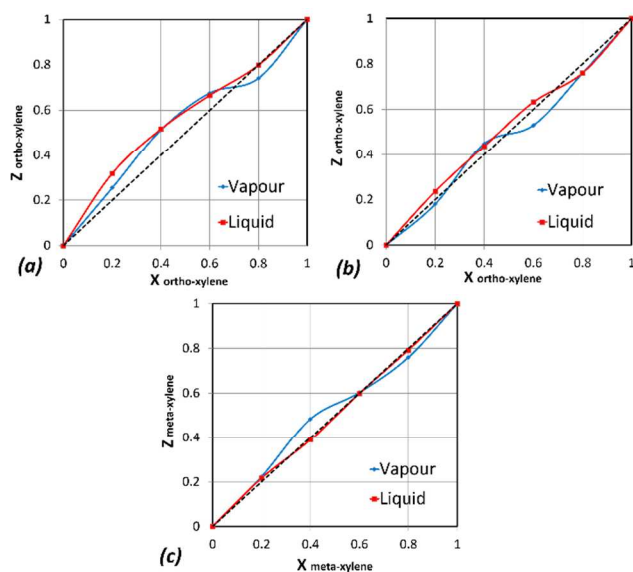

35   **Fig. 5** Selectivity curves for (a) **ox/px**; (b) **ox/mx** and (c) **mx/px**

Discussion

The question to be addressed is why the isoquinoline host under discussion is not selective towards any of the xylene isomers
40 either from liquid or vapour mixtures, while the host bis(isothiocyanato) tetrakis(4-phenylpyridine) nickel (II) has been shown to discriminate efficiently between *ortho-*, *meta-* and *para*-xylenes.[8] Competition experiments between equimolar pairs of two isomers and an equimolar mixture of all three xylenes in
45 the vapour state, show the preference for enclathration to be in the order **ox > mx > px**. We have therefore analysed the non-bonded interactions which occur between a given guest and this host. We have chosen to compare the structures containing the *ortho-* and *meta*-xylene guests, because they are similar in that
50 they both have a host:guest ratio of 1:1, while the structure of *para*-xylene has a host:guest ratio of 1:3. The program Crystal Explorer was employed to calculate the Hirshfeld surfaces of the **ox** and **mx** molecules and their fingerprint plots were generated (Fig. 6)
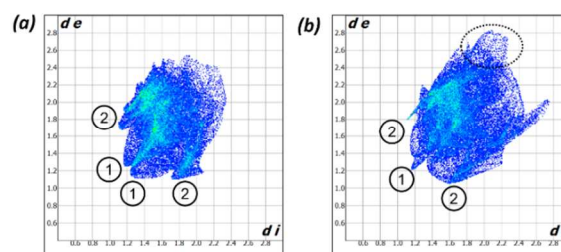

55
Fig. 6 Fingerprint plots for (a) **ox** guest and (b) **mx** guest in their inclusion compounds with bis(isothiocyanato) tetrakis(4-phenylpyridine) nickel (II)

Figure 6a shows the fingerprint plot of the **ox** guest. The two
60 peaks labelled ① are associated with H···H interactions at $(d_i+d_e) \approx 2.48$ Å (57% of the close contacts) while those labelled ② are due to C···H contacts with $(d_i+d_e) \approx 2.87$ Å (37%). In contrast, the **mx** structure, shown in Fig. 6b, has H···H contacts labelled ① at 2.43 Å (68%) and C···H contacts, labelled ② at
65 2.85 Å (28%). The Hirshfeld surface analysis supports the experimental results and explains why the host favours the **ox** guest. Also it demonstrates that the H···H and C···H interactions occur at similar distances, slightly over the sum of the van der Waals radii of 2.40 and 2.90 Å[20] respectively, but there is a
70 greater percentage of C···H interactions in the **ox** structure and the circled area in Fig. 6b shows that there are many long H···H contacts, resulting in a less efficient packing of the **mx** structure.

In addition to the host-guest non-bonded interactions, however, the host with 4-phenylpyridine ligands possesses considerable
75 torsional flexibility in its pyridine and phenyl rings. This fact has been discussed in detail previously.[21] The labelling of the four torsion angles (τ_1, τ_3, τ_5 and τ_7) between the pyridine ring and the thiocyanato ligand (N-Ni-N-C) was carried out cyclically in a manner to yield the minimum in the sum of the square of their
80 differences. The eight torsion angles of each of the three structures have been tabulated and labelled as before[21] (Fig. 7) and their values are summarized in Table 5. It was noted that the differences in the torsion angles τ_3 and τ_4 as well as τ_7 and τ_8 observed in the **mx** structure indicated large rotations of the
85 phenyl ring (Table 5 for **mx**, Δ values in bold) compared with τ_1/τ_2 and τ_5/τ_6 differences. The selectivity for **mx** is less than **ox** but greater than **px**. In the case of **ox**, alternating positive and

negative torsion rotations are observed (τ_1/τ_2 and τ_5/τ_6 negative; τ_3/τ_4 and τ_7/τ_8 positive). This attests to the fact that this is a highly flexible ligand, which easily adapts to the requirement of a given guest, rendering it selective.
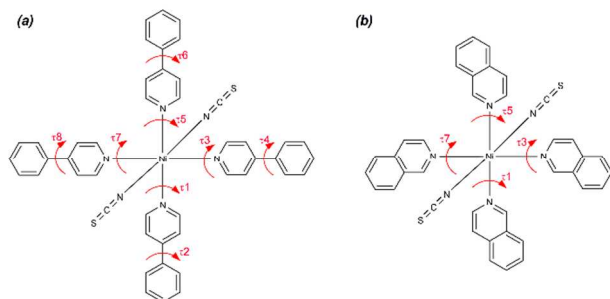

Fig.7 Torsion angles in (a) Ni(NCS)$_2$(4-phenylpyridine)$_4$ and (b) **H**

Table 5 Torsion angles of Ni(NCS)$_2$(4-phenylpyridine)$_4$ in its crystals of xylene isomers.

Guest	τ_1/τ_2	τ_3/τ_4	τ_5/τ_6	τ_7/τ_8
ox	32.4	39.7	34.1	43.9
	45.1	25.7	44.4	31.3
Δ	-12.7	14.0	-10.3	12.8
mx	20.3	20.8	46.6	34.4
	21.8	-29.7	15.5	-30.1
Δ	-1.5	**50.5**	31.1	**64.5**
px	23.0	34.6	40.2	39.7
	34.7	19.2	40.0	27.1
Δ	-11.7	15.4	0.2	12.6

The torsion angles describing the pyridine moieties in the currently investigated host **H** (τ_1, τ_3, τ_5 and τ_7) are remarkably similar to previously analysed compounds. They correspond to the 'four-blade propeller' configuration found in the structures of analogous compounds containing pyridine (**W1**), 4-methyl- (**W2**), 4-vinyl- (**W3**), and 4-phenyl- (**W4**) pyridines. This corresponds to the ++++ configuration described by Lipkowski.[2,22] Table 6 and Fig. 8 show the range of torsion angles for these apohosts, as well as the torsion angles for the currently discussed three structures **H·px**, **H·mx** and **H·ox.** Despite presenting four positively rotated ligands in the isoquinoline host **H**, the torsion angles also indicate two large and two smaller angles. This shows compensation for the interaction of the host with the guest, whereas in the apohost structures no guest is present.

Table 6 Torsion angles τ_1, τ_3, τ_5 and τ_7 for **H** and some typical nickel Werner clathrates where the ligands are pyridine (**W1**), 4-methyl- (**W2**), 4-vinyl- (**W3**), and 4-phenyl- (**W4**) pyridine.

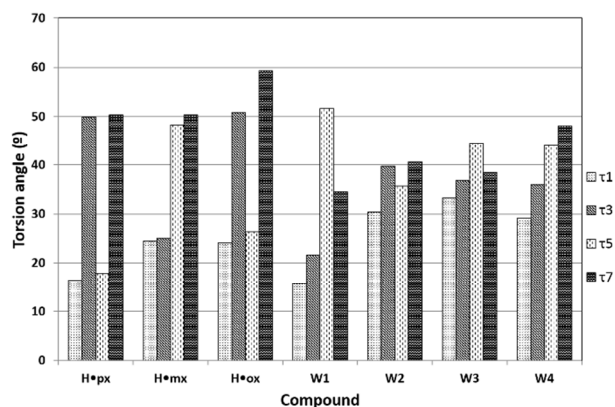| Compound	τ_1 (º)	τ_3 (º)	τ_5 (º)	τ_7 (º)
H•px	16.5	49.9	17.9	50.3
H•mx	24.5	25.1	48.3	50.3
H•ox	24.2	50.8	26.4	59.3
W1	15.7	21.6	51.6	34.5
W2	30.4	39.8	35.7	40.6
W3	33.3	36.8	44.5	38.5
W4	29.2	36.0	43.9	48.0

Fig. 8 Plot of torsion angles of Werner complexes based on values presented in Table 6

Experimental Section

Preparation of Werner clathrate

The host compound, **H**, bis (isothiocyanato) tetrakis (isoquinoline) nickel(II), was prepared by adding stoichiometric quantities of an ethanolic solution of isoquinoline (20 ml, 0.01 M) to an ethanolic solution of nickel-isothiocyanate (5 ml, 0.01 M). Violet crystals of Ni(NCS)$_2$(C$_9$H$_7$N)$_4$ formed immediately and were filtered and allowed to air dry overnight.

Enclathration of any given xylene guest was carried out by dissolving the host in benzene, adding the xylene isomer (**px**, **mx** and **ox**) dropwise and stirring at 60 °C for 30 minutes, cooling and filtering. Crystallisation occurred within 24 hours. Deep blue crystals of **H·px**, **H·mx** and **H·ox** were formed.

Single crystal X-ray analysis

Intensity data of a selected single crystal for compounds **H·px**, **H·mx** and **H·ox** was collected on a Bruker DUO APEX II diffractometer[23] with graphite monochromated Mo K$_{\alpha 1}$ radiation (λ = 0.71073 Å) at 173 K using an Oxford Cryostream 700. Data reduction and cell refinement were performed using *SAINT-Plus*.[24] The space group was determined from systematic absences by *XPREP*.[25] The structure was solved using *SHELXS-97*[26] and refined using full matrix least squares methods in *SHELXL-97*[28] with the aid of the program *X-Seed*.[27] The hydrogen atoms bound to carbon atoms were placed at idealized positions and refined as riding atoms. Diagrams and publication material were generated using *PLATON*,[28] *X-Seed* and *Mercury (3.1).*[29] Crystal data and structure refinement parameters are given in Table 1. CCDC 1041252-1041254 contain the supplementary crystallographic data for structures **H·px**, **H·mx** and **H·ox**. This data can be obtained free of charge *via* www.ccdc.cam.ac.uk/data_request/cif, by e-mailing data_request@ccdc.cam.ac.uk, or by contacting the Cambridge Crystallographic Data Centre, 12 Union Road, Cambridge CB2 1EZ, UK; fax: +44(0)1223-336033. DOI:0.1039/b000000x

Powder X-ray diffraction

Powder X-ray diffraction experiments were carried out on a Bruker D8 diffractometer using Cu K$_\alpha$ radiation. The sample was ground to a fine powder and loaded into an aluminium tray.

Where available these spectra were compared with those determined from the single crystal structures.

Thermogravimetric analysis

Thermal analyses were performed on a TA Q500 instrument from 30 to 350 °C at heating rates from 2, 4, 8, 16 and 32 °C min^{-1} with a purge gas of dry nitrogen flowing at 60 ml min^{-1}. All samples were dried on filter paper and placed in an open pan for thermogravimetric analysis. Sample masses varied from 2 to 5 mg.

Competition experiments

The selectivity of the host for a particular isomer was evaluated using two different procedures and analysing both by headspace gas chromatography. The first was a solid-vapour experiment in which crushed host was exposed to a mixture of two xylene guests in an evacuated chamber at room temperature for 18 hours. The compound was removed from the chamber, dried and placed in a headspace vial for GC analysis. The second method involved crystal formation of the host with guest mixture using the same procedure mentioned above. Crystals were harvested, dried and placed in headspace vials for GC analysis.

Gas chromatography

GC analysis was performed on an Agilent 7890A instrument with Varian CP Wax capillary column (30 m x 250 μm x 0.25μm), nitrogen carrier gas and FID detector with inlet and detector temperatures of 280 °C. Vials were incubated at 50 °C for 10 minutes before injection; oven temperature at 35 °C for 1 minute, followed by a gradient at 10 ° C min^{-1} to 120 ° C for 2 minutes.

Conclusions

A Werner clathrate [Ni(NCS)$_2$(isoquinoline)$_4$] has been synthesised and its properties elucidated. Due to the importance of the xylene isomers in the petroleum industry, *para-, meta-* and *ortho-*xylenes were considered as the guests in this study. Single crystal structures of the host•guest compounds were analysed and the packing established. The analysis of the fingerprint plots revealed the importance of the C-H•••π interactions and unique C-H•••S interactions were observed in the **H•ox** structure.

The non-isothermal technique of Flynn and Wall was used to record the kinetics of thermal decomposition of the three inclusion compounds. Similar plots for the three compounds show initial loss of the guest, followed by two steps, each denoting the mass loss of two isoquinoline ligands.

The selectivity of **H** towards the xylene isomers was determined using two methods, viz. solid vapour sorption and crystallisation from a liquid solution of host and a bimolecular mixture of the guests. The results were analysed using headspace gas chromatography. No significant preference for one of the xylene isomers over the other two was found, showing poor selectivity of this host.

The poor selectivity of this host **H** was compared to that of the related host [Ni(NCS)$_2$(4-phenylpyridine)$_4$]. The success of the latter host was attributed to the torsional flexibility of the phenyl moieties in the ligands. In contrast, the isoquinoline ligands, although containing larger aromatic systems, have no such flexibility and their relative conformation is largely controlled by their *ortho-*hydrogens.

Notes and references

[a] *University of Cape Town, Rondebosch, Cape Town, South Africa. Fax: 27 21 6505419; Tel: 27 21 6505893*
[b] *Cape Peninsula University of Technology, Zonnebloem, Cape Town, South Africa.; Tel: 27 21 4608354; E-mail: bathorin@cput.ac.za*

† Electronic Supplementary Information contains the non-isothermal TG curves for **H•mx** and **H•ox** and the activation energies for **H•mx** and **H•ox**. See DOI: 10.1039/b000000x/

1 W. D. Schaeffer, W. S. Dorsey, D. A. Skinner and C. G. Christian, *J. Amer. Chem. Soc.,*1957, **79**, 5870.
2 J. Lipkowski, in *Inclusion Compounds,* **Vol 1,** Chapter 3, Academic Press, New York, 1984.
3 J. Lipkowski, in *Comprehensive Supramolecular Chemistry,* **Vol 6,** Chapter 20, eds. D.D. MacNicol, F. Toda and R. Bishop, Elsevier Science, Oxford, 1996.
4 D. V. Soldatov, G. D. Enright and J. A. Ripmeester, *Cryst. Growth Des.,* 2004, **4**, 1185.
5 C. J. Adams, M. F. Haddow, D. J.Harding, T. J. Podesta and R. E. Waddington, *CrystEngComm,* 2011, **13**, 4909.
6 S. Wohlert, I. Jess, U, Englert and C. Nather, *CrystEngComm,* 2013, 5326.
7 M. Lusi and L. J. Barbour, *CrystEngComm,* 2014, **16**, 36.
8 M. Lusi and L. J. Barbour, *Angew. Chem. Int. Ed.* 2012, **51**, 3928.
9 E. Batisai, M. Lusi, T. Jacobs and L.J. Barbour, *Chem. Commun.,* 2012, 12171.
10 S. M. Soliman, Z. B. Elzawy, M. A. M. Abu-Youssef, J. Albering, K. Gatterer, L. Öhrström and S. F. A. Kettle, *Acta Cryst.,* 2014, B70, 115.
11 F. Allen, *Acta Crystallogr., Sect. B,* 2002, **58**, 380.
12 P. Baran, M. Boča, R. Boča, A. Krutošíková, J Miklovič, J. Pelikán and J. Tituš, *Polyhedron,* 2005, **24**, 1510.
13 MarvinSketch 14.8.11.0, 2014, ChemAxon (http://www.chemaxon.com)
14 CrystalExplorer (Version 3.1), S. K. Wolff, D. J. Grimwood, J. J. McKinnon, M. J. Turner, D. Jayatilaka and M. A. Spackman, University of Western Australia, 2012.
15 M. A. Spackman and D. Jayatilaka, *CrystEngComm,* 2009, 11, 19.
16 (a) M.A.Spackman and J.J. McKinnon, *CrystEngComm,* 2002, **4**, 378; (b) McKinnon, J.J.; Jayatilaka, D.; Spackman, M.A. *Chem Commun.,* 2007, 3814.
17 M. Đaković, D. Vila-Viçosa, M.J. Calhorda and Z. Popović, *CrystEngComm,* 2011, **13**, 5863
18 J. H. Flynn and L. A. Wall, *Polymer Lett.,* 1966, **4**, 323.
19 L. R. Nassimbeni, *Acc. Chem. Res.,* 2003, 36, 631.
20 A. Bondi, *J.Phys.Chem.,* 1964, **68**, 441.
21 L. R. Nassimbeni, M. L. Niven and M. W. Taylor, *Inorganica Chimica Acta,* 1987, **132**, 67.
22 J. Lipkowski, *J. Mol. Struct.,*1981, **75**, 13.
23 Bruker 2005. APEX2. Version 1.0-27. Bruker AXS Inc., Madison, Wisconsin, USA.
24 Bruker 2004. SAINT-Plus (including XPREP). Version 7.12. Bruker AXS Inc., Madison, Wisconsin, USA.
25 Bruker 2003, XPREP2. Version 6.14. Bruker AXS Inc., Madison, Wisconsin, USA.

26 G. M. Sheldrick, SHELXS-97 and SHELXL-97 Programs for crystal structure determination and refinement. University of Göttingen, 1997.

27 L. J. Barbour, *J. Supramol. Chem.*, 2001, 1, 189.

28 A. L. Spek, PLATON, A Multipurpose Crystallographic Tool, Utrecht University, Utrecht, The Netherlands, 2008.

29 C. F. Macrae, I. J. Bruno, J. A. Chisholm, P. R. Edgington, P. McCabe, E. Pidcock, L. Rodriguez-Monge, R. Taylor, J. van de Streek, P. A. Wood, *J. Appl. Cryst.*, 2008, 41, 466.

Dalton Transactions Accepted Manuscript

Graphical Abstract

Isoquinoline-based Werner clathrates with xylene isomers: Aromatic interactions vs. molecular flexibility

Merrill M. Wicht, Nikoletta B. Báthori[*] and Luigi R. Nassimbeni
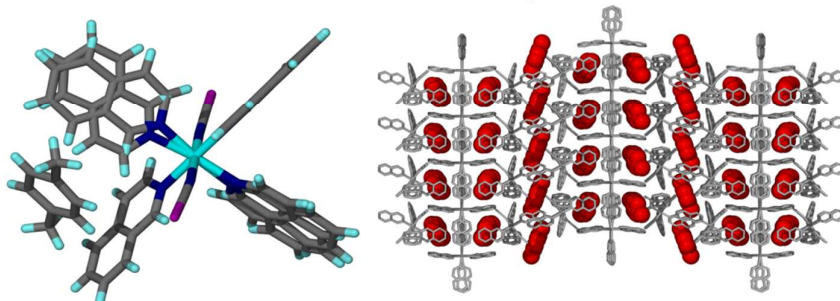
The crystal structure, packing, kinetics and selectivity experiments of the xylene clathrates formed with the Werner complex, bis (isothiocyanato) tetrakis (isoquinoline) nickel(II), is presented.